Macromolecules
ARTICLE

*Macromolecules* **2010**, *43*, 5211–5221 **5211**
DOI: 10.1021/ma1004937

# Controlled/Living *ab Initio* Emulsion Polymerization via a Glucose RAFT*stab*: Degradable Cross-Linked Glyco-Particles for Concanavalin A/*Fim*H Conjugations to Cluster *E. coli* Bacteria

**S. R. Simon Ting, Eun Hee Min,† Per B. Zetterlund,* and Martina H. Stenzel***

*Centre for Advanced Macromolecular Design, School of Chemical Engineering, University of New South Wales (UNSW), Sydney NSW 2052, Australia. † Current address: Photonics and Optical Communications Group, School of Electrical Engineering and Telecommunications, UNSW*

*Received March 8, 2010; Revised Manuscript Received April 30, 2010*

ABSTRACT: Glyco-particles bearing glucose units have been prepared via a one-step controlled/living *ab initio* cross-linking emulsion polymerization of styrene based on self-assembly via a glucose RAFT*stab* (reversible addition−fragmentation chain transfer colloidal stabilizer). The RAFT*stab* was synthesized from the monomer 2-(methacrylamido)glucopyranose (MAG) and the hydrophobic trithiocarbonate RAFT agent *S*-methoxycarbonylphenylmethyl dodecyltrithiocarbonate (MCPDT). In order to obtain glyco-particles stable for biomedical applications, a degradable bis(2-acryloyloxyethyl) disulfide cross-linker (disulfide diacrylate, DSDA) was employed in the emulsion polymerization. The cross-linked glyco-particles were stable in *N*,*N*-dimethylacetamide (DMAc), in contrast to the corresponding non-cross-linked glyco-particles which disintegrate to form linear glycopolymers in solution. The cross-linked particles underwent reductive degradation into the constituent linear (primary) chains upon treatment with 1,4-dithiothreitol (DDT). The bioactivity of the glucose moieties on the surface of the particles was examined using two classes of lectins, namely plant lectin (Concanavalin A, *Canavalia ensiformis*) and bacteria lectin (*fim*H, from *Escherichia coli*). Successful binding was demonstrated, thus illustrating that these particles have potential as "smart" materials in biological systems.

## Introduction

Glyco-particles play a vital role in the biomedical field as their affinity toward lectins could serve as targeting systems in the human body. Lectins are proteins that specifically recognize complementary carbohydrates.[1] These unique interactions between carbohydrates and lectins were discovered and established some time ago by biophysicists and biochemists.[2,3] Reviews on cluster glycoside effects have further fortified the concept of enhanced interactions between polymeric carbohydrates and binding proteins.[4,5] Glyco-particles or linear glycopolymers containing multiple pendant sugars could potentially be used to combat infections, as drug delivery systems, and other biological sensing devices, attributed to the biofunctionality of sugars on the particle surface.[6−11] Hence, there is a desire to improve the techniques used for glyco-particle synthesis. To improve the biofunctionality of the particles when administered in vivo, polymeric glyco-particles need to be stable enough for biomedical applications to overcome low concentrations, various pH changes, and different ionic strengths. Self-assembly of block copolymers with one glycopolymer block into micelles, followed by cross-linking of the micelles, is one possible pathway to generate stable core−shell nanoparticles.[12] However, the preparation is normally carried out in multiple steps as there is a need to construct amphiphilic diblock copolymers for the self-assembly into micelles, then self-assemble the block copolymers, and eventually cross-link the micelles into stable particles.[8,9,13] Alternatively, bioactive core−shell particles can be generated by surface modifications of preformed particles in order for desired carbohydrates or biomolecules to be grafted onto the particles.[14,15] Glyco-particles may also be prepared by conventional radical emulsion copolymerization of a sugar-containing monomer and a hydrophobic monomer, but a significant fraction of sugar-monomer would be embedded within the particle, and particle size control is usually difficult.[16]

Cross-linking of micellar structures is now an established procedure.[8,12,13] However, many cross-linking techniques result in a permanent fixation of particles, and considerations have to be given to the synthetic materials being left in the biological system after the release of drug.[8,17,18] Degradation of the cross-linking points of the micelles can easily be achieved by taking advantage of the environmental conditions that is typical for cell interiors. Because of the acidic and reductive environment in the cell, acid-cleavable micelles and thiol-sensitive micelles have been designed as delivery systems to be stimulated and degraded to release model drugs.[19−26] The resulting low molecular weight linear polymers (typically $< 40\,000$ g mol$^{-1}$) can then be cleared by efficient renal elimination.[27]

Emulsion polymerization provides an avenue for the synthesis of polymer particles[28,29] and is a potential route to functional polymer particles in one single step. Controlled/living radical polymerization (CLRP)[30] enables the synthesis of polymers with well-defined microstructure and can be readily employed to impart functionality. However, it is a far from trivial task to carry out CLRP as an *ab initio* emulsion polymerization as described in recent reviews.[31,32] Perhaps the most successful approach relies on self-assembly of amphiphilic block copolymer formed in situ or amphiphilic (surface active) "control agents" (e.g., reversible addition−fragmentation chain transfer (RAFT) agent),

*Corresponding authors: Fax +61 2 93856250, Tel +61 2 93854331, e-mail p.zetterlund@unsw.edu.au (P.B.Z.); Fax +61 2 93854344, Tel +61 2 93856250, e-mail m.stenzel@unsw.edu.au (M.H.S.).


Published on Web 05/17/2010

**Scheme 1. Schematic of Disulfide Cross-Linked Glyco-Particles Synthesized via the Glucose RAFT*stab* in Emulsion**

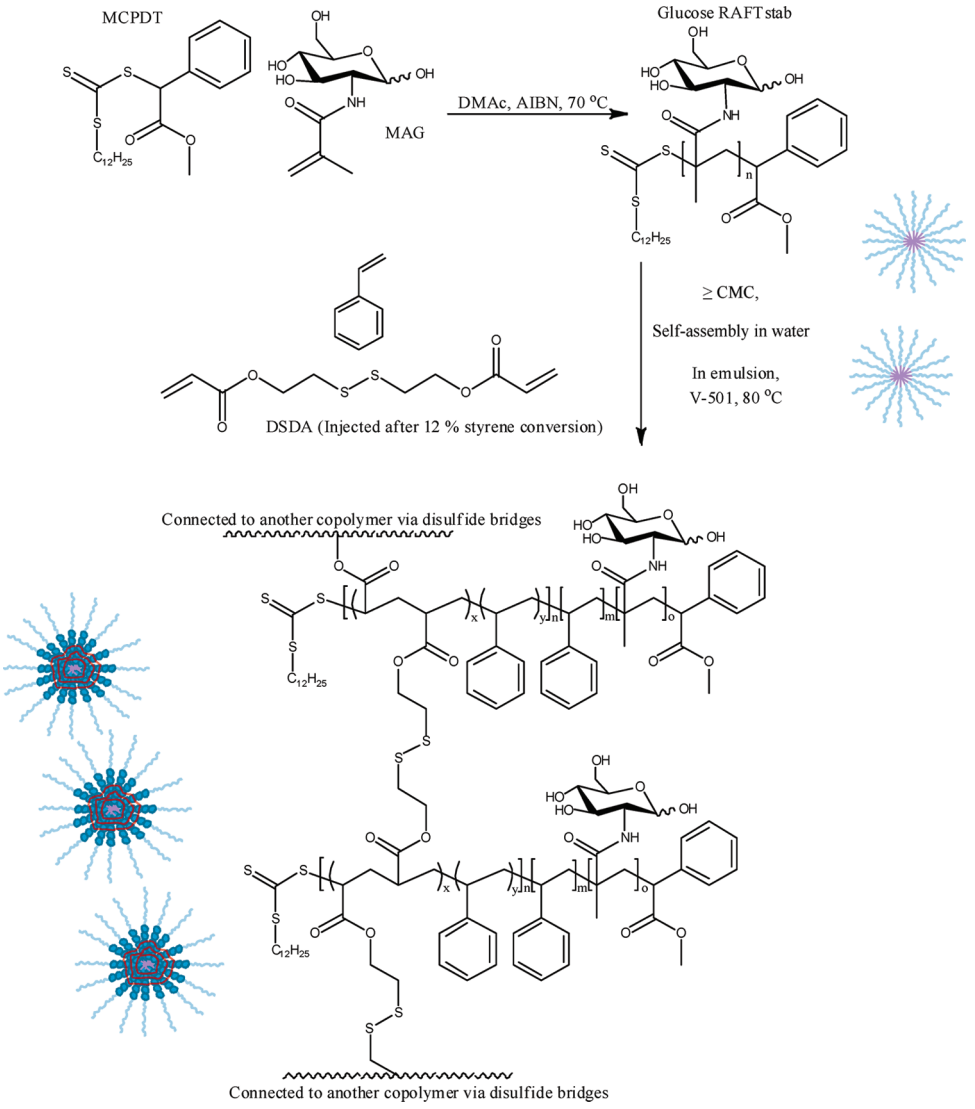


resulting in micelle formation and subsequent particle formation. This surfactant-free approach was initially developed with RAFT[33,34] but has also been implemented using nitroxide-mediated radical polymerization (NMP).[35,36] In the case when RAFT polymerization is employed to form an amphiphilic block copolymer in situ, a monomer feed technique must be employed to ensure the absence of monomer droplets. The presence of monomer droplets prior to micelle formation results in radical entry into monomer droplets followed by polymerization, which in turn leads to colloidal instability and usually poor control/livingness.[31] If the original RAFT agent undergoes micelle formation (e.g., the surface active sodium salt of a low molecular weight trithiocarbonate RAFT agent[37]) or is formed in situ at the very early stage of the polymerization, the polymerization can be performed as a true one-step system where all ingredients are added at the beginning.[37−41]

The synthesis of sugar-containing monomers can be carried out in many ways. The acylation of carbohydrates with acryloyl chloride and methacyloyl chloride and the chemoenzymatic synthesis of carbohydrates are common approaches.[8,42−44] Other methods such as the formation of ester and ether bonds have also been employed; however, most of these methods require the use of deprotection steps after the synthesis of monomer.[45,46]

The aim of the present work has been to develop a process for synthesis of polymeric glyco-particles in a one-pot emulsion polymerization and to subsequently investigate the biological activity of these particles. To this end, a water-soluble sugar-based macroRAFT agent that acts as both mediating and stabilizing agent (RAFT*stab*) has been synthesized and employed in an *ab initio* emulsion polymerization of styrene (St) utilizing the self-assembly concept for particle nucleation (Scheme 1). An unprotected carbohydrate monomer (glucosamine hydrochloride) was selected to avoid deprotection chemistry (Scheme 2). A trithiocarbonate RAFT agent was chosen as it has recently been classified as more biologically suitable than the more established dithioester RAFT agents because polymer synthesized using the latter require purification.[47] The glucose particles were cross-linked by copolymerization with a degradable disulfide cross-linker, thus enabling eventual degradation to the corresponding linear glycopolymers by a reductant (Scheme 3). In summary, the approach presented here aims to eliminate tedious multistep procedures to bioactive nanoparticles. Instead, the feasibility of a simple one-step method will be investigated.

The bioactivities of the glucose sugar moieties on the surface of the latex particles were subsequently screened using ConA (*Canavalia ensiformis*), a glucose and mannose specific binding protein (Scheme 4).[5,48] Further binding ability of the glucose on the particles was examined with a green fluorescence protein (GFP) *Escherichia coli* (*E. coli* DH5α strain).[6,7,49]

**Scheme 2. Synthesis of 2-(Methacrylamido)glucopyranose (MAG) from Glucosamine Hydrochloride and Methacryloyl Chloride**

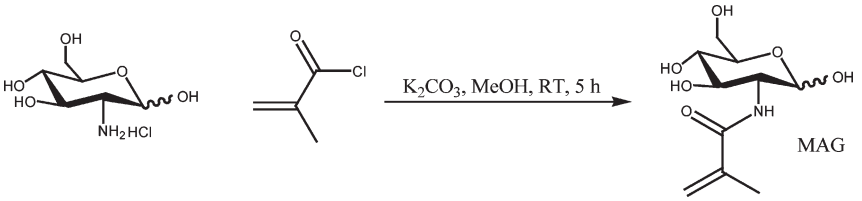


**Scheme 3. Degradation Pathway of Disulfide Core-Cross-Linked Glyco-Particles**

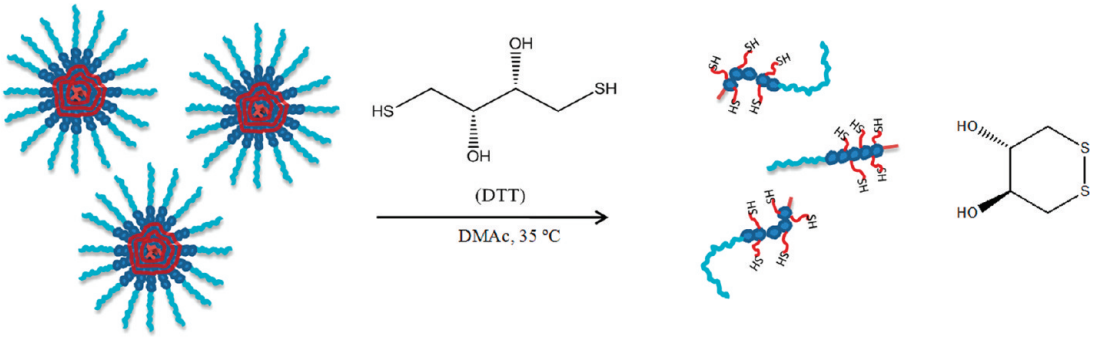


**Scheme 4. Precipitation of Disulfide Core-Cross-Linked Glyco-Particles from Intermicellar Interaction with ConA Lectin**

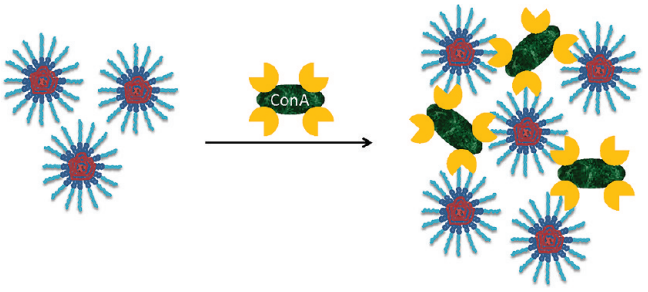


## Experimental Section

**Materials.** 1-Dodecanethiol (≥98%), carbon disulfide (ACS reagent, ≥99.9%), methyl α-bromophenyl acetate (97%), D-(+)-glucosamine hydrochloride (≥99.9%, crystalline), methyl α-D-mannopyranoside (≥99%), methacryloyl chloride (purum, dist., ≥97%), 4,4′-azobis(4-cyanopentanoic acid) (V-501, purum, dist., ≥98.0%), fluorescein *o*-acrylate (97%), *N,N*-dimethylacetamide for high-performance liquid chromatography (DMAc, HPLC grade, CHROMASOLV PLUS, ≥99.9%), and Concanavalin A (ConA, Type IV, lyophilized powder) from *Canavalia ensiformis* (Jack bean) were purchased from Aldrich and used directly. 2,2′-Azobis(2-methylpropionitrile) (AIBN) from Aldrich was crystallized twice in methanol before used. Styrene (St, *ReagentPlus*, ≥99.9%) and methyl methacrylate (MMA, 99%) were also brought from Aldrich and was de-inhibited by passing through an alumina column before used. Potassium hydroxide (97.0%), dichloromethane (DCM, 99.5%), methanol (99.8%), sodium chloride (salt, 99.9%), and chloroform (99.8%) were all purchased from Univar and used without further treatment. Molecular sieves (4 Å) from Univar were first activated at a temperature of 200 °C before used. Potassium carbonate (≥99.0%) from May and Baker was used directly. Triethylamine (TEA, purum, 99.0%) provided by Riedel-de Haën, bis(2-hydroxyethyl) disulfide (BHEDS, technical grade) from Aldrich, and acryloyl chloride (96%) from Alfa Aesar were used directly from the bottles. 1,4-Dithiothreitol (DDT) from Pierce was used directly. 0.01 M phosphate-buffered saline (PBS) at pH 7.4 was prepared by dissolving the powder from a sachet purchased from Sigma into 1 L of distilled water.

**Synthesis.** *Synthesis of 2-(Methacrylamido)glucopyranose (MAG).* Typically, glucosamine hydrochloride (10.0 g, $4.64 \times 10^{-2}$ mol) and potassium carbonate (6.41 g, $4.64 \times 10^{-2}$ mol) were vigorously stirred to dissolve in 250 mL of methanol in a 500 mL single neck round-bottom flask. The flask was later cooled to −10 °C using an acetone/ice bath before methacryloyl chloride (4.36 g, $4.17 \times 10^{-2}$ mol) was added dropwise into the mixture with vigorous stirring. The mixture was stirred at −10 °C for 30 min and left to react for another 3 h at room temperature. The crude mixture was filtered through a sintered funnel with vacuum suction to remove precipitated salt, and the filtrate was concentrated under reduced pressure to off-white slurry. The slurry was loaded onto a column chromatography for purification with dichloromethane/methanol (ratio 4:1) as the eluent. The white solid exit the column with the $R_f$ value of 0.33, with 58% conversion obtained gravimetrically. $^1$H NMR ($D_2O$, 300 MHz) $\delta$ (ppm): 1.87 (s, 3H, $CH_3$), 3.35−3.95 (m, 6H, sugar moiety 6 × C*H*), 4.70−4.72 (d, 0.43H, anomeric $\beta$-C*H*), 5.15−5.16 (d, 0.57H, anomeric α-C*H*), 5.41 (s, 1H, Me−C=C*H*H), 5.64 (s, 1H, Me−C=CH*H*).

*Synthesis of S-Methoxycarbonylphenylmethyl Dodecyltrithiocarbonate (MCPDT).* 1-Dodecanethiol (6.41 g, $3.17 \times 10^{-2}$ mol) was suspended in 43 mL of distilled water and cooled in an ice bath. This was followed by the addition of potassium hydroxide (1.82 g, $3.25 \times 10^{-2}$ mol) before 6.5 mL of carbon disulfide was introduced dropwise into the suspension. A yellow emulsion was observed during the addition of carbon disulfide. Methyl α-bromophenyl acetate (5.0 g, $2.19 \times 10^{-2}$ mol) was eventually added dropwise into the yellow emulsion, and a condenser was attached onto the single neck round-bottom flask, after which the reaction vessel was heated to 80 °C for 12 h. Upon cooling, the water phase was separated from the organic phase and washed with methylene chloride (3 × 20 mL). The yellow solution of all the organic phases were concentrated under reduced pressure to give a yellow oil. The yellow oil was further purified through a column using toluene as the eluent with the product exiting at an $R_f$ value of 0.8. The combined fractions were dried under reduced pressure and high vacuum to yield a bright yellow oil and upon cooling in the fridge gave a bright yellow solid. The reaction conversion (60%) was obtained using $^1$H NMR by observing the integrals from the proton shift of 4.51 to 5.75 ppm. ESI-MS ($CH_2Cl_2$) calculated for $C_{22}H_{34}O_2S_3 + Ag^+$ $m/z$, 533.08; found, $m/z$ 533.30. $^1$H NMR ($CDCl_3$, 300 MHz) $\delta$ (ppm): 0.81 (t, 3H, $CH_3$), 1.19 (s, 18H,

$CH_3-C_9H_{18}-(CH_2)_2-S$), 1.61 (m, 2H, $CH_2-CH_2-S$), 3.26 (t, 2H, $CH_2-S$), 3.68 (s, 3H, $O-CH_3$), 5.75 (s, 1H, $S-CH-(Ph)-C(O)=O$), 7.27 (m, 5H, $ArH_5$). $^{13}C\{^1H\}$ NMR ($CDCl_3$, 75.5 MHz) $\delta$ (ppm): 14.53 (1C, $CH_3$), 23.09 (1C, $CH_3-CH_2$), 28.23, 29.30, 29.48, 29.74, 29.82, 29.94, 30.02, 30.11 (8C, $C_8H_{16}-CH_2-S$), 32.32 (1C, $CH_3-CH_2-CH_2$), 37.72 (1C, $CH_2-S$), 53.60 (1C, $O-CH_3$), 58.19 (1C, S-CH(Ph)−C(O)=O), 125.70, 128.62, 129.15, 129.29, 129.44, 133.64 (6C, ArC), 169.90 (1C, $CH(Ph)-C(O)=O$), 222.40 (1C, $S=C(S)-S$).

*Synthesis of Bis(2-Acryloyloxyethyl) Disulfide Cross-Linker (Disulfide Diacrylate, DSDA)*. 4 Å molecular sieves were first transferred into a 500 mL single neck round-bottom flask in a glovebox. Anhydrous tetrahydrofuran, THF (133.4 g, 1.85 mol), was introduced into the round-bottom flask at nitrogen atmosphere. This was followed by anhydrous triethylamine (36.3 g, $3.59 \times 10^{-1}$ mol). BHEDS (7.7 g, $5.00 \times 10^{-2}$ mol), was initially diluted with 5 mL of anhydrous THF and later injected into the reaction mixture. The magnetic stirred round-bottom flask sealed with a rubber septum was chilled to 0 °C using an ice bath. The reaction started when acryloyl chloride (20.0 g, $2.21 \times 10^{-1}$ mol) was injected into the round-bottom flask over a period of 15 min. After stirring at 0 °C for 2 h, the reaction mixture was slowly warmed to room temperature and left stirring for another 22 h. The resulted reaction mixture was filtered through a sintered funnel, washed with saturated brine solution for three times, and washed with distilled water for three times before dried with reduced pressure. The dark orange viscous liquid was purified through a silica column with chloroform as the eluent. The light yellow oil exited the column with an $R_f$ value of 0.4, yielding 62% conversion via gravimetry. $^1H$ NMR ($CDCl_3$, 300 MHz) $\delta$ (ppm): 2.91 (t, 4H, $2 \times S-CH_2$), 4.36 (t, 4H, $2 \times CH_2-O$), 5.77−5.81 (dd, 2H, $2 \times CH=CHH$), 6.02−6.11 (dd, 2H, $2 \times CH=CHH$), 6.34−6.40 (dd, 2H, $2 \times CH=CHH$).

*Homopolymerization of MAG with MCPDT (RAFTstab Synthesis)*. In a typical experiment, MAG (2.80 g, $1.13 \times 10^{-2}$ mol) was first measured into a 50 mL round-bottom flask containing a magnetic stirring bar. 11 mL of DMAc was subsequently added to dissolve the MAG. Before MCPDT ($1.61 \times 10^{-1}$ g, $3.77 \times 10^{-4}$ mol) was introduced into the above solution, it was first measured in a separate vial and dissolved in 500 $\mu$L of DMAc to aid transfer. AIBN ($7.70 \times 10^{-3}$ g, $4.71 \times 10^{-5}$ mol) was finally measured and added into the solution, and the flask was seal with a rubber septum. The flask was purged with nitrogen for 40 min and transferred into a preheated oil bath set at 60 or 70 °C. Aliquots were taken at different time intervals and dissolved in $D_2O$ to monitor the polymerization kinetics. MAG monomer conversions were calculated by comparing the vinylic proton at 5.64 ppm of the monomer with the six protons at 3.35−3.95 ppm from both the monomer and polymer. The final polymer from the crude mixture was dialyzed (membrane cutoff of 1000 g mol$^{-1}$) against distilled water overnight with water changed every 6 h to remove unreacted MAG. The lyophilized sample was further purified from any organics via extraction using diethyl ether (three times).

The homopolymerization resulted in 79% monomer conversion after 19 h. SEC analysis gave a molecular weight of $M_n$ = 13 500 g mol$^{-1}$, PDI = 1.30 ($M_{n,th}$ = 6300 g mol$^{-1}$).

*Emulsion Polymerization of Styrene via the Glucose RAFTstab*. Normally, the glucose RAFT*stab* (0.26 g, $4.50 \times 10^{-5}$ mol, $M_{n,th}$ = 6300 g mol$^{-1}$, PDI = 1.30) was first dissolved in 3.0 mL of distilled water in a 10 mL round-bottom flask with the help of a magnetic stirrer. Subsequently, V-501 ($2.50 \times 10^{-3}$ g, $9.0 \times 10^{-6}$ mol) was dissolved in the above mixture by rapid stirring at low temperature. Finally, styrene (0.94 g, $9.0 \times 10^{-3}$ mol) was added into the flask, which was sealed with a rubber septum. The emulsion was thoroughly degassed with some agitation (to allow the formation of a uniform heterogeneous phase for efficient degassing) for 50 min to remove any oxygen. The polymerization was carried out at 80 °C in an oil bath. Aliquots were taken and quenched at different reaction times to obtain the conversions gravimetrically, the evolution of the average particle diameter, and the molecular weights. The latex particles were purified by drying in vacuum at room temperature.

*Cross-Linking Emulsion Copolymerization of DSDA with Styrene via the Glucose RAFTstab*. Glucose RAFT*stab* (0.2 g, $3.18 \times 10^{-5}$ mol, $M_{n,th}$ = 6300 g mol$^{-1}$, PDI = 1.30) was first dissolved into 2.12 mL of distilled water, followed by dissolving V-501 ($1.78 \times 10^{-3}$ g, $6.36 \times 10^{-6}$ mol) with rapid stirring at low temperature. Styrene (0.66 g, $6.37 \times 10^{-3}$ mol) was added to the above solution; the round-bottom flask was sealed with a rubber septum and degassed in nitrogen with some agitation (to allow the formation of a uniform heterogeneous phase for efficient degassing) for 50 min. The polymerization started when the flask was immersed into a preheated oil bath at 80 °C. After 217 min, a degassed mixture of DSDA ($8.36 \times 10^{-2}$ g, $3.19 \times 10^{-4}$ mol) with 1 mg of fluorescein *o*-acrylate was injected into the emulsion reaction. Aliquots were taken and quenched at different reaction times for analyses. The latex particles were purified by drying in vacuum at room temperature.

*Degradation of Core-Cross-Linked Glyco-Particles*. Degradation experiments were performed using online-DLS measurements. Cross-linked glyco-particle solutions were first prepared by dissolving 2 mg of purified polymers into 1 mL of DMAc. 1.0 M of DTT solution was prepared by dissolving 7.7 mg into 50 $\mu$L of DMAc. Before DTT was added to the solution containing glyco-particles, an initial measurement was made. The degradation test started when 25 $\mu$L of 1.0 M of DTT solution was added into the above prepared particles solution in a 1 cm quartz cuvette. This was followed by vigorous shaking, and immediately the cuvette was returned into the holding block with the temperature set at 35 °C for measurements for a duration of 35 min.

*Canavalia ensiformis Turbidimetry Binding Assay*. 1 mg mL$^{-1}$ of ConA was prepared in 0.01 M phosphate-buffered saline (PBS) at pH 7.4. 300 $\mu$L of this lectin solution was transferred into a masked quartz semimicrocell and placed into the holding block of the UV−vis spectrophotometer for temperature equilibration at 25 °C, and a baseline was subsequently taken. A solution of 200 $\mu$L containing the glucose ligand diblock copolymer, cross-linked glyco-particles, or RAFT*stab* in PBS solution (922 $\mu$M per glucose residue) was added to the cuvette containing the lectin solution. The solution in the cuvette was thoroughly mixed using a pipet and immediately returned into the holding block where an absorbance at 420 nm was recorded for 12 min. A competitive binding assay with 1-methyl α-D-mannopyranoside (100 mg mL$^{-1}$ prepared in PBS, pH 7.4) was later conducted by gently introducing 20 $\mu$L of the mannose solution into the ConA conjugated glyco-particles without mixing and the absorbance was recorded over 12 min.

*Bacteria Adhesion Studies*. *Escherichia coli* (GFP *E. coli* DH5α strain) was used for adhesion studies. Bacteria were grown in lysogeny broth (LB) medium to stationary phase (O.D. 0.8) by overnight incubation at 37 °C in the dark. 300 $\mu$L aliquots were collected in Eppendorf tubes and centrifuged at 13 000 rpm for 3 min. The supernatant was then replaced with the diluted emulsion mixture containing latex glyco-particles or the RAFT*stab* dissolved in distilled water ($1.87 \times 10^5$ glucose residue). The samples were vortexed for 5 s and left to settle for 30 min at room temperature of about 25 °C, after which the samples were gently shaken and 10 $\mu$L of the samples were pipetted onto a glass slide with a glass coverslip placed on it for examination under the microscope. Control experiments were also conducted by replacing the supernatant with only distilled water without the glycopolymers. Competitive binding assays were conducted by transferring 2 or 5 $\mu$L of 1-methyl α-D-mannopyranoside solution (100 mg mL$^{-1}$ prepared in distilled water) into two glyco-particles/bacteria suspensions 70 $\mu$L each in Eppendorf tubes; suspensions were obtained from the above adhesion experiments. Samples were vortexed for 5 s

and left to settle for 30 min. Aliquots of 10 $\mu$L from each samples were mounted on a glass slide with a glass coverslip over the samples for examinations under the microscope.

**Analysis.** *Nuclear Magnetic Resonance* (*NMR*) *Spectroscopy*. All NMR spectra were recorded using a Bruker DPX-300 spectrometer with a resonance frequency of 300.2 MHz for $^1$H nuclei at 25 °C. MAG monomer and PMAG (RAFT*stab*) were analyzed using deuterated water as solvent.

*Size Exclusion Chromatography* (*SEC*). Molecular weight distributions were determined by SEC with a Shimadzu modular system with *N*,*N*-dimethylacetamide (DMAc) (0.03% w/v LiBr, 0.05% BHT stabilizer) at 50 °C with a flow rate of 1.0 mL min$^{-1}$. The system incorporated a DGU-12A solvent degasser, a LC-10AT pump, and a CTO-10A column oven and was equipped with a RID-10A refractive index detector. Polymer Laboratories (PL) 5.0 $\mu$m bead-size guard column (50 × 7.5 mm) followed by four 300 × 7.8 mm linear PL columns ($10^5$, $10^4$, $10^3$, and 500 Å) were used to separate the samples. The system was calibrated using narrow PL polystyrene standards ranging from 500 to $10^6$ g mol$^{-1}$. Filtered polymer samples using 0.45 $\mu$m RC filters were injected at concentrations of 2 mg mL$^{-1}$. Chromatograms were processed using Cirrus 2.0 software from PL.

*Dynamic Light Scattering* (*DLS*). Particles sizes were determined using a Malvern Zetasizer nano ZS with a laser of 4 mW (He−Ne), $\lambda$ = 632 nm, 173°, backscatter. Critical micelle concentrations (cmc) were measured by first fixing the attenuation to 7, and a series of concentrations between the RAFT*stab* and distilled water were measured starting from the highest concentration followed by gradual dilutions with automatic run time. Emulsion aliquots taken at different conversions were measured straight after dilution to ~1 mg mL$^{-1}$ with automatic run time. Degradation experiments were measured with the average of 5 runs at 15 s for each run with the attenuation fixed at 5. The mean diameter was obtained from the arithmetic mean using the number distributed diameter of each particle size.

*UV−vis Spectrophotometer*. A UV−vis spectrophotometer (Cary 300) equipped with a temperature controller was used for the turbidimetric assay of the ligand/protein conjugation. Absorbance data were recorded at 420 nm for 12 min at 1.2 Hz.

*Transmission Electron Microscopy* (*TEM*). TEM micrographs were obtained using a JEOL 1400 transmission electron microscope at an accelerating voltage of 100 kV. The samples were prepared by casting the diluted emulsion mixture (~1 mg mL$^{-1}$) onto a copper grid coated with Formvar.

*Fluorescent Microscopy*. Bacteria adhesions images were taken with a Leica DC100 digital camera attached to a Leica DMLB epi-fluorescence, with 400 times magnification, using Leica's IM 50 as imaging software.

## Results and Discussion

**Synthesis of 2-(Methacrylamido)glucopyranose (MAG).** As part of the design of the glucose RAFT*stab*, a sugar-containing monomer (MAG) not requiring protection chemistry was synthesized. Nucleophilic substitution (Schotten−Baumann reaction) at the carbonyl group of methacryloyl chloride with the primary amine of the glucosamine hydrochloride catalyzed by potassium carbonate was conducted in methanol. This reaction was initially conducted in water, however, due to the poor solubility of methacryloyl chloride in water, and to minimize side reactions and byproducts, methanol was eventually used as solvent (glucosamine hydrochloride, methacyloyl chloride, and potassium carbonate exhibit good solubility in methanol).[43] Column chromatography of the crude mixture could be conducted significantly more efficiently when methanol was the reaction solvent due to the much lower amount of byproducts. Characterization

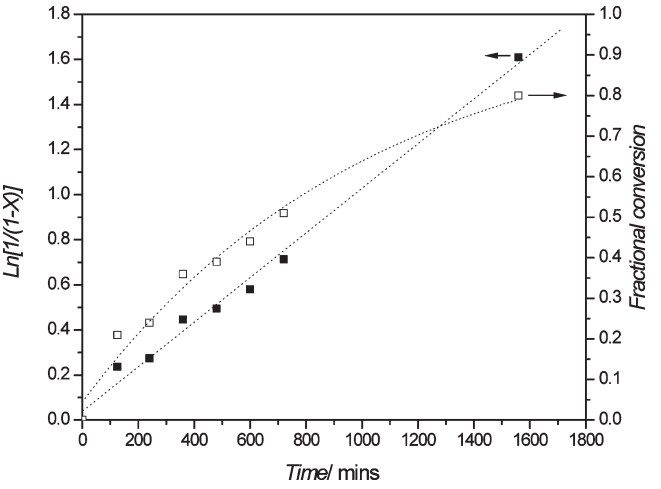


**Figure 1.** Conversion and pseudo-first-order plot of the polymerization of MAG with MCPDT RAFT agent at 70 °C in DMAc. [MAG] = 4.73 × $10^{-1}$ mol L$^{-1}$, [MCPDT] = 2.78 × $10^{-3}$ mol L$^{-1}$, and [AIBN] = 5.57 × $10^{-4}$ mol L$^{-1}$.

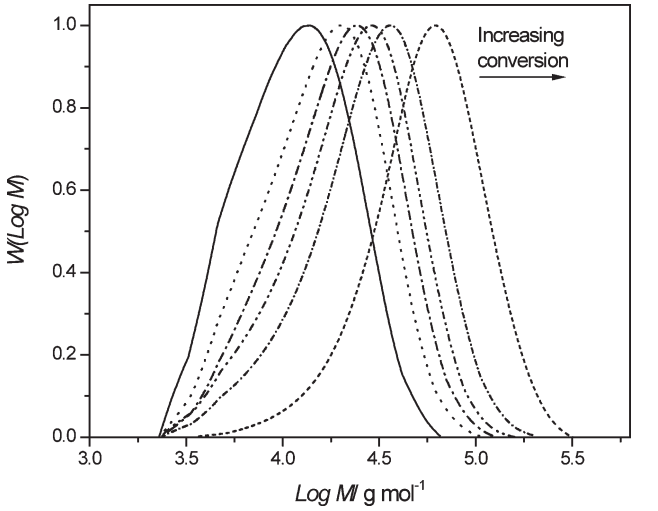


**Figure 2.** Molecular weight distributions of MAG homopolymerization with MCPDT RAFT agent at 70 °C in DMAc at various conversions (21, 24, 36, 44, 51, and 80%). [MAG] = 4.73 × $10^{-1}$ mol L$^{-1}$, [MCPDT] = 2.78 × $10^{-3}$ mol L$^{-1}$, and [AIBN] = 5.57 × $10^{-4}$ mol L$^{-1}$.

by $^1$H NMR using deuterated water showed good agreement with the structure of MAG [Figure SI-1 (Supporting Information)].

**RAFT*stab* Synthesis.** The amphiphilic nature of the RAFT*stab* was attained by homopolymerization of MAG using the highly hydrophobic RAFT agent *S*-methoxycarbonylphenylmethyl dodecyltrithiocarbonate (MCPDT), specifically designed to have a long alkyl chain in the Z-group. The synthesis of MCPDT was carried out following a procedure similar to a previously reported approach (Scheme 2 and Figure SI-1).[8]

Polymerization of methyl methacrylate (MMA) at 60 °C mediated by MCPDT was carried out to confirm its ability to control a model radical polymerization, yielding an experimental molecular weight (MW) calibrated relative to polystyrene ($M_n$) = 19 100 g mol$^{-1}$ and $M_w/M_n$ = 1.42 at 94% conversion. The obtained polymer was subsequently purified and extended with MMA to yield $M_n$ = 45 700 g mol$^{-1}$ and $M_w/M_n$ = 1.20 (Figure SI-2). A similar RAFT agent, *S*-methoxycarbonylphenylmethyl methyltrithiocarbonate

(MCPMT), has previously been successfully employed in the polymerization of MMA.[50]

Polymerization of MAG mediated by MCPDT and initiated by AIBN in DMAc was carried out at 70 °C for RAFT*stab* synthesis. Polymerization was also carried out at 60 °C for comparison (Figure SI-3). The first-order plot at 70 °C was approximately linear (Figure 1). The MWDs shifted to higher MW with increasing conversion (Figure 2), but the values of $M_w/M_n$ did not decrease with increasing conversion (contrary to what is customary in CLRP), remaining approximately constant at 1.3−1.4 at both 70 and 60 °C (Figure 3 and Figure SI-4, respectively). The relatively high $M_w/M_n$ values most likely originate in the chain transfer constant being relatively low. The Z-group of MCPDT, a dodecanethiol group, reduces the stability of the intermediate radical compared to the often used phenyl group, thus lowering the addition rate coefficient for addition of the propagating radical to the C=S bond.[50] In addition, methacrylate and methacrylamide (in this work) monomers generally have low chain transfer constants.[50,51] Moreover, the R-group of MCPDT results in formation of a secondary radical on fragmentation, which may cause the initial RAFT agent to have a lower chain transfer coefficient than the in situ generated polymeric counterpart (which generates a tertiary radical), hence resulting in $M_n > M_{n,th}$ at low conversion and $M_n \approx M_{n,th}$ at high conversion (Figure 3 and Figure SI-4).

The RAFT*stab* ($PMAG_{23}$-MCPDT) synthesized, to be used in the subsequent emulsion polymerizations, had $M_n$ = 13 500 g mol$^{-1}$ ($M_{n,th}$ = 6300 g mol$^{-1}$) and $M_w/M_n$ = 1.30. The polymerization was conducted in a separate experiment with [MAG]/[RAFT] = 50 at 70 °C. To confirm the livingness, a successful chain extension polymerization of the RAFT*stab* with MMA was performed in DMAc (Figure SI-5).

The degree of polymerization of the MAG segment in the RAFT*stab* was targeted to obtain a PMAG macroRAFT agent with a cmc well below the polymerization conditions. The cmc values of different PMAG macroRAFT agents were determined by monitoring the scattering intensity of the RAFT*stab* solutions at different concentrations. Following the method of Charleux et al.,[38] Figure 4 depicts the scattering intensity vs RAFT*stab* concentration (Debye plot[52]) for $PMAG_{23}$-MCPDT at 25 and 65 °C, yielding cmc = 14.5 mM at 65 °C and cmc = 15.2 mM at 25 °C, which falls within the range of reported values for similar amphiphilic species.[38,40,53,54] Cmc is a function of temperature, and high temperature can result in the disintegration of micelles.[13] However, the cmcs were very similar at both temperatures. PMAG macroRAFT agents such as $PMAG_{66}$-MCPDT with higher molecular weights have cmc values above the concentrations employed in the polymerization, and they are therefore deemed inadequate.

**Emulsion Polymerization of St with RAFT*stab*.** Before the radical cross-linking emulsion copolymerization of St and DSDA via the glucose RAFT*stab*, a detailed investigation into the corresponding emulsion homopolymerization of St was undertaken. Preliminary results showed that conducting the emulsion polymerizations above cmc of the RAFT*stab*, as expected, is crucial. Polymerization below the cmc results in sometimes bimodal molecular weight distributions or very broad molecular weight distributions.

Emulsion polymerization (Table 1, experiment 1) was subsequently conducted with the RAFT*stab* $PMAG_{23}$-MCPDT concentration above cmc of 14.5 mM (Figure 4).

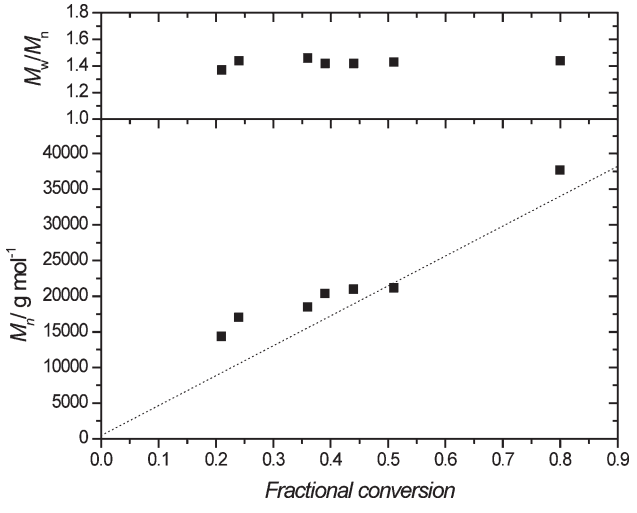


**Figure 3.** Molecular weight and $M_w/M_n$ vs conversion of the homopolymerization MAG with MCPDT RAFT agent at 70 °C, with the dotted line as the theoretical molecular weight. [MAG] = 4.73 × 10$^{-1}$ mol L$^{-1}$, [MCPDT] = 2.78 × 10$^{-3}$ mol L$^{-1}$, and [AIBN] = 5.57 × 10$^{-4}$ mol L$^{-1}$.

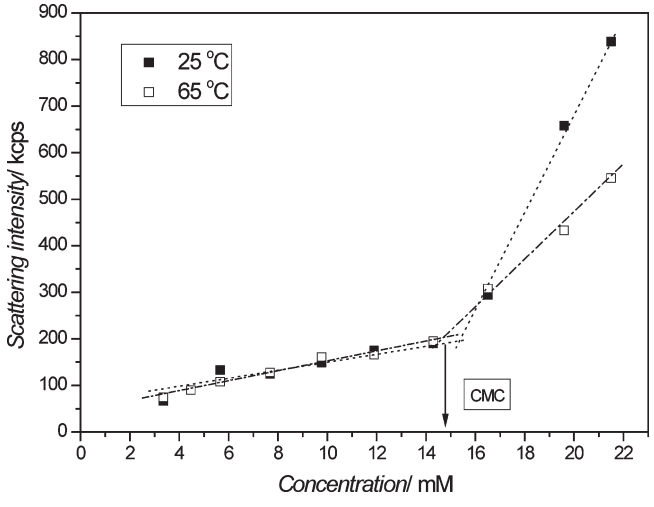


**Figure 4.** Scattering intensity vs RAFT*stab* ($PMAG_{23}$-MCPDT) concentration in water at 25 and 65 °C from dynamic light scattering analysis.

**Table 1. Reaction Parameters and Latex Characterizations of the *ab Initio* Emulsion Polymerization of St and the Radical Cross-Linking *ab Initio* Emulsion Copolymerization of St and Bis(2-acryloyloxyethyl) Disulfide (DSDA) via the Glucose RAFT*stab* ($PMAG_{23}$-MCPDT) at 80 °C[a]**

| expt | wt % monomer in the latex | [Raft*stab*] (mol L$^{-1}$) | [V-501] (mol L$^{-1}$) | [monomer][b]/ [RAFT*stab*] | time (h) | conv (%) | $M_{n,th}$ (g mol$^{-1}$) | $M_n$ (g mol$^{-1}$) | $M_w/M_n$ | $D_h$ (nm); (PDI) |
|---|---|---|---|---|---|---|---|---|---|---|
| 1 | 23.9 | 1.5 × 10$^{-2}$ | 3.0 × 10$^{-3}$ | 200 | 21 | 83 | 23 600 | 38 500 | 1.65 | 81 (0.250) |
| C1[c] | 14.1 | 7.5 × 10$^{-3}$ | 2.5 × 10$^{-3}$ | 200 | 6 | | | gel | gel | gel |
| C2[d] | 26.0 | 1.5 × 10$^{-2}$ | 3.0 × 10$^{-3}$ | 200 | 20 | 81 | | 660 000 | 1.33 | 57 (0.129) |

[a] All concentrations measured with respect to the volume of distilled water used only. [b] $[Monomer]_0$ corresponds to the initial concentration of St or both St and DSDA in the case of cross-linking emulsion polymerization. [c] Cross-linking emulsion polymerization of St carried out with 10 mol % of DSDA added at the start of polymerization. [d] Cross-linking emulsion polymerization of St carried out with 5 mol % of DSDA injected after 12% St conversion.

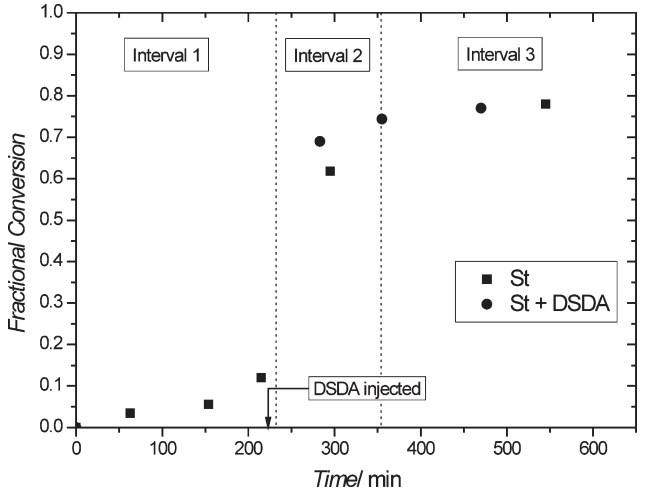


**Figure 5.** Conversion and pseudo-first-order plot of the emulsion polymerization of St with the glucose RAFT*stab* at 80 °C and the cross-linking emulsion copolymerization of St and DSDA (injected at 217 min, 12 % St conversion). [See Table 1, experiment 1 (■) and C2 (●).]

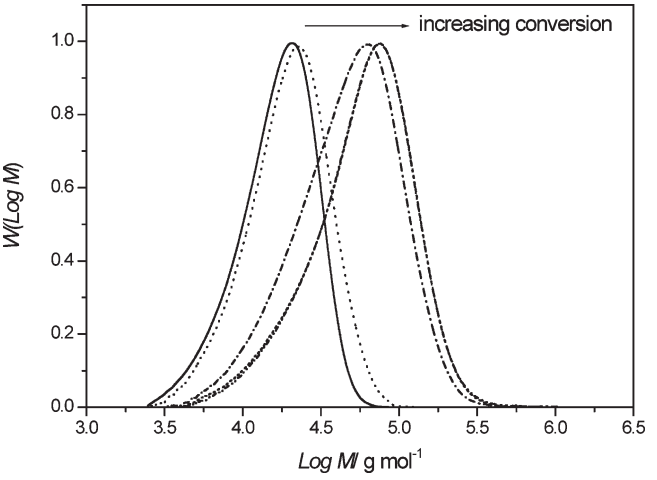


**Figure 6.** Molecular weight distributions of emulsion polymerization of St with glucose RAFT*stab* at various conversions (0, 6, 61, 78, and 83 %; 78 and 83 % almost overlap) at 80 °C. (See Table 1, experiment 1.)

The conversion vs time plot is typical of an *ab initio* emulsion polymerization, displaying intervals 1−3.[28] Interval 1, where particle nucleation occurs and the number of particles increases, appears to end at ∼20−30% conversion, followed by a region with close to constant polymerization rate (interval 2), and finally interval 3 where the rate decreases as monomer is gradually depleted. Figure 6 depicts the MWDs, showing a clear shift in MWs from the initial RAFT*stab* with increasing conversion, but with some low MW tailing. The MWDs were properly normalized with respect to the total amount of polymer to enable quantitative comparison (Figure SI-6), revealing more clearly that some fraction of the initial RAFT*stab* (and/or RAFT*stab* having undergone minor chain extension) remained at high conversion. The values of $M_n$ increased almost linearly with conversion, although $M_n \gg M_{n,th}$ (due to the difference in hydrodynamic volume of polystyrene, used for calibration, and the glycopolymer[9]), and $M_w/M_n$ increased gradually from 1.3 to 1.6 (Figure 7).

The particle size increased linearly with conversion while the PDI dropped from 0.6 to 0.2 (Figure 8). Transmission

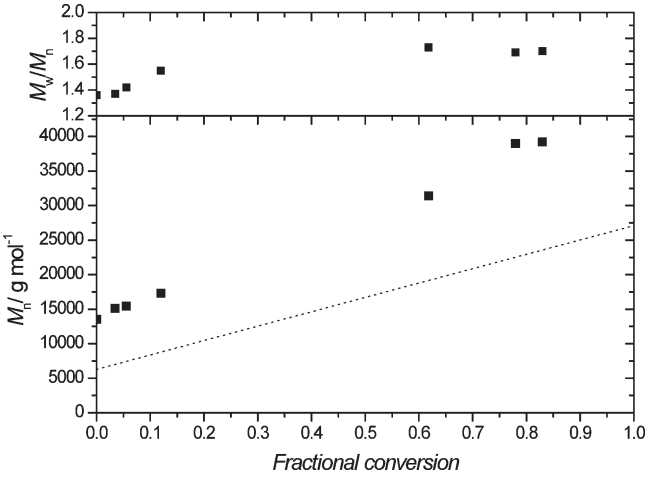


**Figure 7.** Molecular weight and $M_w/M_n$ vs conversion of the emulsion polymerization of St with glucose RAFT*stab* at 80 °C with the dotted line as the theoretical molecular weight. (See Table 1, experiment 1.)

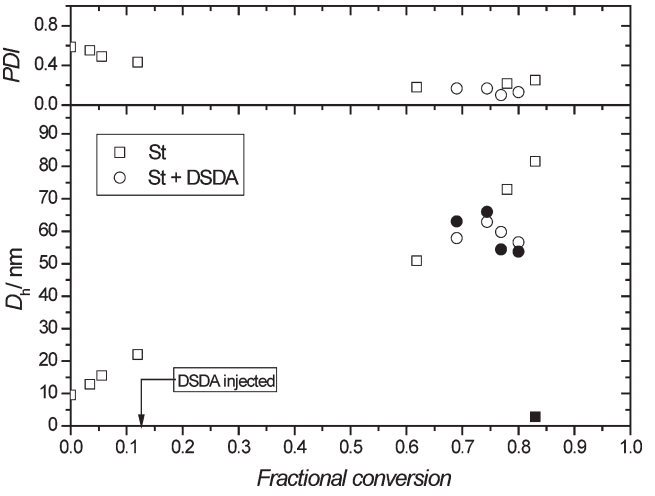


**Figure 8.** Dynamic light scattering measurements of particle diameter ($D_h$) and PDI of glyco-particles at different conversions in the emulsion polymerization of St and the emulsion copolymerization of St and DSDA (injected at 217 min, 12% St conversion) via the glucose RAFT*stab*. The solid symbols, (●) and (■), represent the respective particles purified and redissolved in DMAc.

electron micrographs (TEMs) revealed particles with high definition with the core displaying dark shadows signifying highly dense particles, which is typical of a polystyrene core (Figure 9). The initial "particle" size was very small, ∼10 nm, corresponding to actual micelles. The increase in particle size observed up to high conversion, much more significant and lasting to higher conversion than in a conventional *ab initio* emulsion polymerization,[28] would most likely be caused by slow micellar nucleation accompanied by some micelle dissociation, whereby the thus available "extra" RAFT*stab* would stabilize growing particles.[41,54] However, the conversion−time data suggest interval 1 ends at 20−30% conversion, therefore indicating that some coagulation also contributed to the increase in particle size at higher conversions. A fairly high initial number of micelles would mean that not all micelles become polymer particles, and the nucleation process would extend to significant conversion, which would in turn cause broadening of the MWD (increase in $M_w/M_n$) in the form of low-MW tailing, as observed experimentally

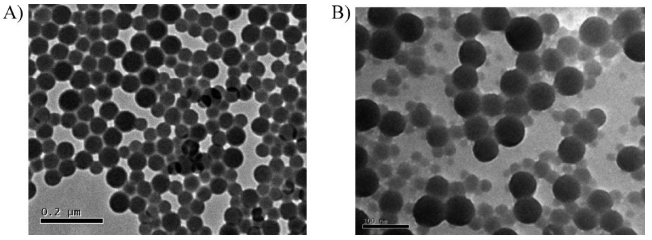


**Figure 9.** Transmission electron microscope images of latex glyco-particles generated from emulsion polymerization of St via the glucose RAFT*stab* at 83% conversion (A) and disulfide core-cross-linked glyco-particles at 81% conversion (B). Scale bars are 0.2 $\mu$m for image A and 100 nm for image B.

(Figure 6). The only polymer chains (i.e., RAFT*stab*) able to grow are the ones located in nucleated micelles (polymer particles). Low-MW tailing may also be partially caused by "dead" RAFT*stab* species, i.e., "RAFT*stab* chains" that do not contain a RAFT moiety at the chain end.

**Cross-Linking Emulsion Copolymerization of St and DSDA with RAFT*stab*.** Having optimized the emulsion polymerization of St, the same basic recipe was employed for synthesis of cross-linked particles using the cross-linking agent DSDA at 80 °C. A similar disulfide-based methacrylate cross-linker has recently been employed in RAFT solution polymerization by Armes and co-workers.[55] Cross-linking emulsion polymerization of St was first carried out with 10 mol % DSDA (relative to St) introduced at the beginning of the polymerization. However, after ~6 h, macroscopic gelation occurred (Table 1 experiment C1). In an attempt to overcome this problem, the amount of DSDA was reduced to 5 mol % and was injected into the vessel after 217 min (~12% conversion), corresponding to the point when significant nucleation had occurred toward the end of interval 1. This approach resulted in a stable emulsion without macroscopic gelation (Table 1, experiment C2). The conversion vs time plot is similar to the corresponding non-cross-linking polymerization, although the absence of data at low to intermediate conversion precludes further analysis (Figure 5). The particle size appears to go through a maximum near 75% conversion (Figure 8). The decrease in particle size observed after 75% conversion may be related to polymer shrinkage associated with cross-linking, although the approximate decrease of 50 vol % (between 75 and 79% conversion) appears too large for this to be the only reason. However, the data may contain fairly significant experimental error (as is common in DLS measurements of this type), and these results should be treated with caution.

A small amount of fluorescein *o*-acrylate (0.8 mol % relative to DSDA) was added with the DSDA in order for the particles to be visualized when applied in vitro. Figure 10 shows the stability of the un-cross-linked and the fluorescent-tagged cross-linked glyco-particles left to stand over a month. Addition of purified particles to DMAc (a good solvent for both St and MAG) allows confirmation of their cross-linked structure as they remained intact without disintegrating to the corresponding primary chains. As the overall monomer conversion increases, purified cross-linked glyco-particles followed the same trend (reduction in size) when redispersed in DMAc when compared to the original cross-linked particles dispersed in water. Dissolution of the non-cross-linked particles in DMAc resulted in a clear solution with $D_h$ of 4 nm (typical for linear polymers of this MW). Particles synthesized from cross-linking emulsion copolymerization of St/DSDA and emulsion polymerization of St resulted in very stable particles in aqueous medium, the

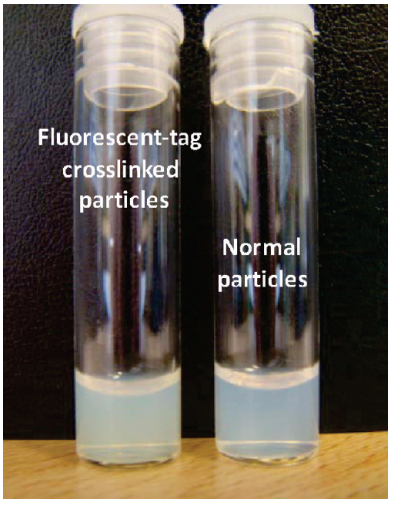


**Figure 10.** Comparison of latex glyco-particles after dilution 100 times in distilled water from final original emulsions and after settling over a month, with and without disulfide cross-linked/fluorescent tagged.

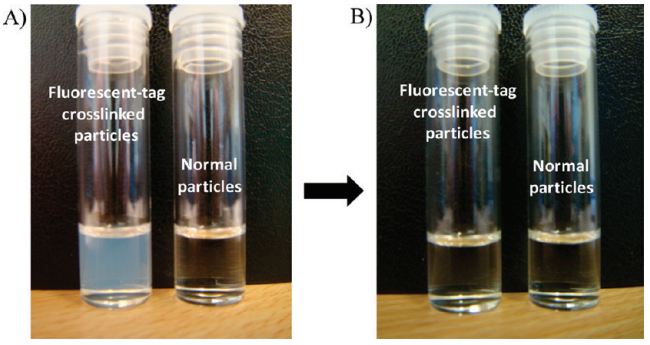


**Figure 11.** Comparison of latex glyco-particles after purification at a concentration of 2 mg $mL^{-1}$ in DMAc, with and without disulfide cross-linked/fluorescent tagged (A) and cross-linked particles treated with DTT for 1 h (B).

particles were still homogenously dispersed in the medium after 1 month (Figure 10). TEM images show that spherical particles were obtained both with and without the cross-linker (Figure 9). However, the particle size distribution appears to be somewhat less uniform for the cross-linked particles.

**Degradation of Core-Cross-linked Latex Particles.** Biological releases of therapeutics in drug carriers are crucial when administered in vivo; hence, the studies on the rate of degradation of polymeric carriers need to be conducted. The aim is to generate particles that are stable in the bloodstream but start degrading rapidly once they are taken up by the cells, where a reductive environment is prevalent.

Reduction reaction, involving scission of disulfide bonds, can be carried out with a thiol reagent (reductant). Degradation of the cross-linked particles into their constituent primary chains was achieved using 1,4-dithiothreitol (DDT) as reducing agent. The cleavage of disulfide bonds was monitored by measuring the scattering intensity and $D_h$ of the cross-linked glyco-particles using dynamic light scattering. DMAc was chosen as solvent as it has the ability to dissolve both the polystyrene and glycopolymer blocks once the disulfide bridges have been cleaved. Sufficient cross-linking was ensured when the glyco-particles were dissolved in DMAc; a very diluted milky solution was observed with the $D_h$ size of 56 nm (Figures 11 and 12). Two different

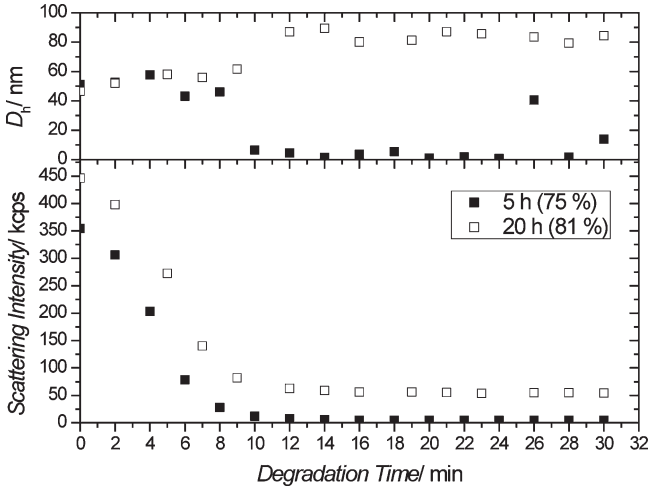


**Figure 12.** Scattering intensity and hydrodynamic diameter vs degradation time during treatment of cross-linked glyco-particles (75 and 81% monomer conversion; polymerization times 5 and 20 h) with DTT in DMAc.

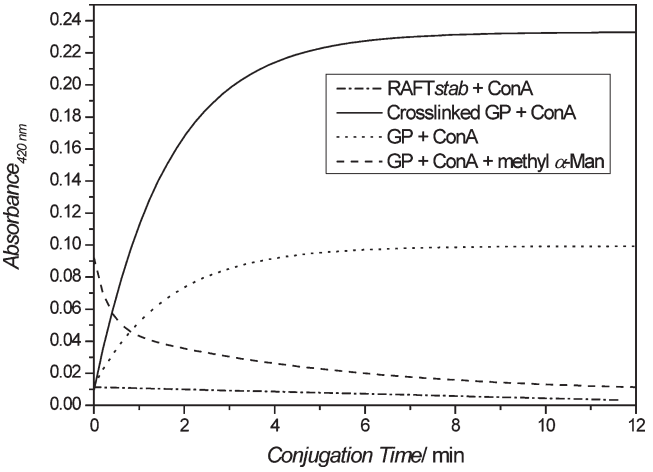


**Figure 13.** Turbidimetry assay of glyco-particles ("GP" in figure)/ cross-linked glyco-particles synthesized via the emulsion polymerization with ConA association binding, RAFT*stab*/ConA association binding, and the dissociation competitive assay of the glyco-particles with ConA after the addition of methyl α-D-mannopyranoside.

cross-linked particles were used in this experiment: one from the final emulsion mixture (see Table 1, experiment C2) when left overnight for polymerization for 20 h (81% conversion) and another was the aliquot taken after 5 h of polymerization (75% conversion) from the same experiment. A reduction in scattering intensity for both core-cross-linked particles was observed, with the particles with 75% conversion reducing to near zero intensity after 10 min and the particles with 81% conversion reducing to 9 times less scattering intensity than the original particles. Further inspections allow more conclusions as the particle sizes from the lower conversion gave values (~4 nm) that correspond to the disintegration into primary chains after reduction of disulfide bridges (Figure 12). However, experimental error may have resulted in the sudden increase in particles size of the glyco-particles at 26 min (Figure 12). Glyco-particles obtained after 20 h did not degrade completely. Formation of permanent cross-links as a result of chain transfer events with the disulfides might have prevented complete degradation of these particles.[23] The decreasing scattering intensity suggests the decomposition of a significant fraction of cross-links. Interestingly, the remaining particles have diameters bigger than the original particles, which may indicate that the remaining particles have only a loose network structure in the core with free thiol groups, which probably promote swelling of the core and thus an increase in size.

**Turbidimetric Binding Assay.** Bioactivity of the glyco-particles was tested using turbidimetric assay via UV/vis spectroscopy.[9,56] The rate of receptor clustering among cells and other biological molecules is a vital parameter in biological systems. The influence of the epitope density on a biological specimen with their binding protein is normally assessed using turbidimetric assays.[57,58] Concanavalin A (ConA), a lectin specific for binding glucose and mannose, was used to investigate the interactions between ConA and the glucose moieties on the surface of the latex particles. Turbidimetric assay was utilized measuring the changes in absorbance at a wavelength of 420 nm during the ConA/glucose interactions. Scheme 4 depicts the clustering and precipitation of latex particles due to intermicellar cross-linking via ConA, a tetrameric binding protein. The RAFT*stab* ($PMAG_{23}$-MCPDT), the latex glucose particles (From Table 1, experiment 1), and the core-cross-linked latex glucose particles (from Table 1, experiment C2) were tested regarding their ability to form clusters with ConA. The rate of complexation between ConA and its ligand depends heavily on the density of the multivalent ligand.[57] In this case, cross-linked latex particles display a clustering rate much higher than the non-cross-linked particles (Figure 13). The density of the multivalent glucose ligand was the same for both cases as the glucose RAFT*stab* used was of the same degree of polymerization ($PMAG_{23}$-MCPDT); furthermore, the concentrations of both ligand solutions (cross-linked particles and non-cross-linked particles) were kept constant. The lower clustering rate displayed by the non-cross-linked particles could be caused by the higher chain dynamics. In contrast, the contracted structure upon cross-linking causes a more brushlike structure of the glycopolymers chains on the surface. It has previously been reported that rigid scaffolds for sugars are entropically favorable to enhance binding.[10]

The aggregates formed by the glucose latex particles and the ConA were later treated with an excess of methyl α-D-mannopyranoside, a competitive monodentate ligand. The competitive binding assay leads to the decrease of the absorbance as mannose, being a stronger ligand for ConA, reverses the binding of glucose particles with ConA (Figure 13).[58] Further experiments with only the linear glucose RAFT*stab* ($PMAG_{23}$-MCPDT) did not result in any visible complexation with ConA (Figure 13). The low binding by the glucose RAFT*stab* may be the result of insufficient numbers of glucose pendant groups on the polymer backbone. The interaction between one glucose moiety and ConA is—in contrast to the stronger conjugation of mannose to ConA—very weak. This is even more pronounced when essential ions such as $Ca^{2+}$ and $Mn^{2+}$ are absent in the buffer solution to allow optimum interactions with ConA.[59] The weakness is not compensated by the 23 glucose repeating units present in the RAFT*stab*. This observation emphasizes even more the strong multivalent effect displayed by the nanoparticles prepared.

**Bacteria Adhesion Studies.** Because of the *fim*H protein carried by the type 1 fimbrae in *E. coli*, interactions between the proteins on the *E.coli* bacteria and glycopolymers are possible.[7] *Fim*H is a lectin that possesses carbohydrate recognition domains (CRD), and it has high affinity binding with mannose ($K_d$ = 2.3 $\mu$M) and glucose ($K_d$ = 9.24 mM).[60] By blocking the binding sites of the bacteria using multivalent glycopolymers with either mannose or

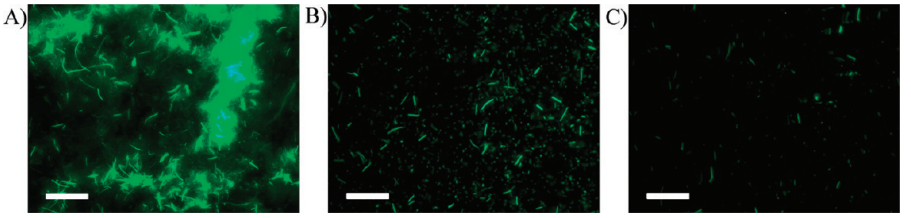


**Figure 14.** Fluorescent microscopy images of GFP *E. coli* mixed with latex glyco-particles without the addition of competitive ligand (A), with 0.01 M methyl α-D-mannopyranoside (B), and with 0.03 M methyl α-D-mannopyranoside (C). Scale bars = 10 μm for all three images.

glucose, the attachment of infectious bacteria onto healthy cells can be prevented. This avenue can also potentially promote dedifferentiation of swarmer cells, hence offering new strategies in modulating the bacteria's multicellular behavior.[11] Figure 14A show a clear aggregation displayed by the formation of bacteria−glycopolymer complex, with high fluorescent patches after mixing the GFP *E. coli* cells with the glyco-particles (from Table 1, experiment C2). Fluorescent images were very similar when compared between non-cross-linked (from Table 1, experiment 1) and cross-linked glyco-particles. Images were taken with the same batch of GFP *E. coli* cells with a measured optical density (OD) of 8; hence, the amounts of cells per volume sample when mixed with the polymeric ligands (RAFT*stab*, un-cross-linked glyco-particles and cross-linked glyco-particles) were approximately equal. In addition, successful aggregation by the *E. coli* cells gave distinct precipitation upon optical inspection in the Eppendorf tubes. Results show that the aggregation of *E. coli* cells was aided by the multivalent ligands provided by the glyco-particles. Control experiment carried out with the same condition but without the glyco-particles did not show aggregation when compared to Figure 14A (Figure SI-7). Preliminary experiments were performed using the same glucose residue concentrations as in the turbidimetric assay, but *E. coli* cells did not show sign of aggregations. The concentrations required were higher than the concentrations used during the turbidimetric assay, as considerations such as the accessibility of the glucose moieties with respect to ConA (plant lectin) receptor and the *fim*H receptor (bacteria lectin) from *E. coli* are very different.[1] Experiments were also conducted by mixing the GFP *E. coli* with the linear precursor (RAFT*stab*). The resulting aggregations among the *E. coli* cells were limited when compared to those mixed with glyco-particles (Figure SI-7).

Competitive binding assays were again tested using 1-methyl α-D-mannopyranoside, a monodendate ligand. Two experiments with different concentrations of competitive ligands were mixed with the bacteria/glyco-particles complex. A concentrated solution of 1-methyl α-D-mannopyranoside in distilled water was prepared in order to pipet minimum volume of competitive ligands into the complex for comparison without disturbing the concentration of cells in the mixtures of complexes. 1-methyl α-D-mannopyranoside as a stronger monodentate ligand compete now with the glycopolymer for binding sites on *E. coli* and as a result lead to the disassociation of the network formed by the glycopolymer. Figure 14B reveals that some residual complexes were still remaining but significantly diminished. Higher concentrations of competitive ligands dissolved the complex completely as the GFP *E. coli* cells spread further apart (Figure 14C).

## Conclusions

One-pot synthesis of glycopolymers by controlled/living RAFT mediated *ab initio* emulsion polymerization, employing a surface active glucose based RAFT*stab*, provide a convenient technique toward bioactive synthetic latex glyco-particles. The RAFT*stab*, based on 2-methacrylamido glucopyranose monomer, was used in the self-assembly based cross-linking *ab initio* emulsion polymerization of styrene. A disulfide cross-linker was used to enable reductive degradation of the cross-linked particles into the constituent linear (primary) chains.

The bioactivity of the latex glyco-particles was examined using two classes of lectins: Concanavalin A (plant lectin, *Canavalia ensiformis*) extracted from Jack bean and *fim*H (bacteria lactin) from green fluorescence protein (GFP) *Escherichia coli* (*E. coli* DH5α strain). Results reveal that the glucose functionalities remain bioactive after being processed into glyco-nanoparticles. Because of the affinity enhancements displayed by carbohydrates molecules and their binding to lectins, these glyco-particles have potential as recognition devices, delivery systems, or aggregating bacteria in the biological system.[2,5,12] The optimized glucose RAFT*stab* provides a platform for other biologically active carbohydrates such as mannose or galactose to be easily converted into their respectively RAFT*stab*. Degradation of the particles after scission of the disulfide (cross-linker) bridges would result in linear low molecular weight polymer and thus facilitate renal elimination.

**Acknowledgment.** The authors thank the Australian Research Council (ARC) for financial support (DP0771155) and the Centre for Advanced Macromolecular Design (CAMD) for support. The authors are very thankful for the use of the laboratory and the fluorescent microscope at the Centre for Marine Bio-Innovation, School of Biotechnology and Biomolecular Sciences (BABS), UNSW. The electron microscopy unit in UNSW is also acknowledged. S. R. S. Ting and E. H. Min appreciate the help from the personnel at BABS namely, S. A. Rice and L. H. Yee for the discussions on *E. coli* work, A. Pham for the assistance in the laboratory, and Y. J. Jeon for the discussions and providing the GFP *E. coli* DH5α strain. M. H. Stenzel acknowledges an ARC Future Fellowship.

**Supporting Information Available:** $^1$H NMR characterizations of MAG and MCPDT; SEC analysis of solution polymerization controlled using MCPDT RAFT agent with kinetic studies at 60 °C and SEC analysis of solution polymerization controlled using RAFT*stab*; conversion normalized response SEC traces of emulsion polymerization of styrene; and fluorescent images of GFP *E. coli* control experiment and bacteria incubated with RAFT*stab*. This material is available free of charge via the Internet at http://pubs.acs.org.

**Note Added after ASAP Publication.** This article posted ASAP on May 17, 2010. The Supporting Information title and Figure SI-1 have been revised. The correct version posted on May 28, 2010.

## References and Notes

(1) Lis, H.; Sharon, N. *Chem. Rev.* **1998**, *98*, 637–674.
(2) Lee, R. T.; Lee, Y. C. *Glycoconjugate J.* **2001**, *17*, 543–551.
(3) Sharon, N.; Lis, H. *Science* **1989**, *246*, 227–34.

(4) Lundquist, J. J.; Toone, E. J. *Chem. Rev.* **2002**, *102*, 555–578.
(5) Pieters, R. J. *Org. Biomol. Chem.* **2009**, *7*, 2013–2025.
(6) Pasparakis, G.; Alexander, C. *Angew. Chem., Int. Ed.* **2008**, *47*, 4847–4850.
(7) Pasparakis, G.; Cockayne, A.; Alexander, C. *J. Am. Chem. Soc.* **2007**, *129*, 11014–11015.
(8) Ting, S. R. S.; Gregory, A. M.; Stenzel, M. H. *Biomacromolecules* **2009**, *10*, 342–352.
(9) Ting, S. R. S.; Min, E.-H.; Escale, P.; Save, M.; Billon, L.; Stenzel, M. H. *Macromolecules* **2009**, *42*, 9422–9434.
(10) Mammen, M.; Chio, S.-K.; Whitesides, G. M. *Angew. Chem., Int. Ed.* **1998**, *37*, 2754–2794.
(11) Lamanna, A. C.; Kiessling, L. L. *ACS Chem. Biol.* **2009**, *4*, 828–833.
(12) Stenzel, M. H. *Macromol. Rapid Commun.* **2009**, *30*, 1603–1624.
(13) Stenzel, M. H. *Chem. Commun.* **2008**, 3486–3503.
(14) Gu, W.; Chen, G.; Stenzel, M. H. *J. Polym. Sci., Part A: Polym. Chem.* **2009**, *47*, 5550–5556.
(15) Ting, S. R. S.; Nguyen, T. L. U.; Stenzel, M. H. *Macromol. Biosci.* **2009**, *9*, 211–220.
(16) Abeylath, S. C.; Turos, E. *Carbohydr. Polym.* **2007**, *70*, 32–37.
(17) Zhang, L.; Katapodi, K.; Davis, T. P.; Barner-Kowollik, C.; Stenzel, M. H. *J. Polym. Sci., Part A: Polym. Chem.* **2006**, *44*, 2177–2194.
(18) Zhang, L.; Nguyen, T. L. U.; Bernard, J.; Davis, T. P.; Barner-Kowollik, C.; Stenzel, M. H. *Biomacromolecules* **2007**, *8*, 2890–2901.
(19) Bulmus, V.; Chan, Y.; Nguyen, Q.; Tran, H. L. *Macromol. Biosci.* **2007**, *7*, 446–455.
(20) Chan, Y.; Bulmus, V.; Zareie, M. H.; Byrne, F. L.; Barner, L.; Kavallaris, M. *J. Controlled Release* **2006**, *115*, 197–207.
(21) Chan, Y.; Wong, T.; Byrne, F.; Kavallaris, M.; Bulmus, V. *Biomacromolecules* **2008**, *9*, 1826–1836.
(22) Zhang, L.; Bernard, J.; Davis, T. P.; Barner-Kowollik, C.; Stenzel, M. H. *Macromol. Rapid Commun.* **2008**, *29*, 123–129.
(23) Zhang, L.; Liu, W.; Lin, L.; Chen, D.; Stenzel, M. H. *Biomacromolecules* **2008**, *9*, 3321–3331.
(24) Cavallaro, G.; Campisi, M.; Licciardi, M.; Ogris, M.; Giammona, G. *J. Controlled Release* **2006**, *115*, 322–334.
(25) Kakizawa, Y.; Harada, A.; Kataoka, K. *Biomacromolecules* **2001**, *2*, 491–497.
(26) Jiang, X.; Liu, S.; Narain, R. *Langmuir* **2009**, *25*, 13344–13350.
(27) Duncan, R. *Nat. Rev. Cancer* **2006**, *6*, 688–701.
(28) Gilbert, R. G., *Emulsion Polymerization: A Mechanistic Approach*; Academic Press: London, 1995.
(29) Nomura, M.; Tobita, H.; Suzuki, K. Emulsion polymerization: Kinetic and mechanistic aspects. In *Polymer Particles*; Okubo, M., Ed.; Springer: Berlin, 2005; Vol. *175*, pp 1−128.
(30) Braunecker, W. A.; Matyjaszewski, K. *Prog. Polym. Sci.* **2007**, *32*, 93–146.
(31) Zetterlund, P. B.; Kagawa, Y.; Okubo, M. *Chem. Rev.* **2008**, *108*, 3747–3794.
(32) Cunningham, M. F. *Prog. Polym. Sci.* **2008**, *33*, 365–398.
(33) Ferguson, C. J.; Hughes, R. J.; Pham, B. T. T.; Hawkett, B. S.; Gilbert, R. G.; Serelis, A. K.; Such, C. H. *Macromolecules* **2002**, *35*, 9243–9245.
(34) Ferguson, C. J.; Hughes, R. J.; Nguyen, D.; Pham, B. T. T.; Gilbert, R. G.; Serelis, A. K.; Such, C. H.; Hawkett, B. S. *Macromolecules* **2005**, *38*, 2191–2204.
(35) Delaittre, G.; Nicolas, J.; Lefay, C.; Save, M.; Charleux, B. *Soft Matter* **2006**, *2*, 223–231.
(36) Dire, C.; Magnet, S.; Couvreur, L.; Charleux, B. *Macromolecules* **2009**, *42*, 95–103.
(37) Stoffelbach, F.; Tibiletti, L.; Rieger, J.; Charleux, B. *Macromolecules* **2008**, *41*, 7850–7856.
(38) Rieger, J.; Stoffelbach, F.; Bui, C.; Alaimo, D.; Jerome, C.; Charleux, B. *Macromolecules* **2008**, *41*, 4065–4068.
(39) Bernard, J.; Save, M.; Arathoon, B.; Charleux, B. *J. Polym. Sci., Part A: Polym. Chem.* **2008**, *46*, 2845–2857.
(40) Rieger, J.; Osterwinter, G.; Bui, C.; Stoffelbach, F.; Charleux, B. *Macromolecules* **2009**, *42*, 5518–5525.
(41) Wang, X. G.; Luo, Y. W.; Li, B. G.; Zhi, S. P. *Macromolecules* **2009**, *42*, 6414–6421.
(42) Albertin, L.; Cameron, N. R. *Macromolecules* **2007**, *40*, 6082–6093.
(43) Pearson, S.; Allen, N.; Stenzel, M. H. *J. Polym. Sci., Part A: Polym. Chem.* **2009**, *47*, 1706–1723.
(44) Ting, S. R. S.; Granville, A. M.; Quemener, D.; Davis, T. P.; Stenzel, M. H.; Barner-Kowollik, C. *Aust. J. Chem.* **2007**, *60*, 405–409.
(45) Ohno, K.; Izu, Y.; Yamamoto, S.; Miyamoto, T.; Fukuda, T. *Macromol. Chem. Phys.* **1999**, *200*, 1619–1625.
(46) Xiao, N.-Y.; Li, A.-L.; Liang, H.; Lu, J. *Macromolecules* **2008**, *41*, 2374–2380.
(47) Chang, C.-W.; Bays, E.; Tao, L.; Alconcel, S. N. S.; Maynard, H. D. *Chem. Commun.* **2009**, 3580–3582.
(48) Schuster, M. C.; Mortell, K. H.; Hegeman, A. D.; Kiessling, L. L. *J. Mol. Catal. A: Chem.* **1997**, *116*, 209–216.
(49) Min, E.; Wong, K. H.; Stenzel, M. H. *Adv. Mater.* **2008**, *20*, 3550–3556.
(50) Perrier, S.; Takolpuckdee, P.; Westwood, J.; Lewis, D. M. *Macromolecules* **2004**, *37*, 2709–2717.
(51) Barner-Kowollik, C.; Quinn, J. F.; Nguyen, T. L. U.; Heuts, J. P. A.; Davis, T. P. *Macromolecules* **2001**, *34*, 7849–7857.
(52) Debye, P. *J. Appl. Phys.* **1944**, *15*, 338–42.
(53) Fuguet, E.; Rafols, C.; Roses, M.; Bosch, E. *Anal. Chim. Acta* **2005**, *548*, 95–100.
(54) Ganeva, D. E.; Sprong, E.; De Bruyn, H.; Warr, G. G.; Such, C. H.; Hawkett, B. S. *Macromolecules* **2007**, *40*, 6181–6189.
(55) Rosselgong, J.; Armes, S. P.; Barton, W.; Price, D. *Macromolecules* **2009**, *42*, 5919–5924.
(56) Geng, J.; Mantovani, G.; Tao, L.; Nicolas, J.; Chen, G.; Wallis, R.; Mitchell, D. A.; Johnson, B. R. G.; Evans, S. D.; Haddleton, D. M. *J. Am. Chem. Soc.* **2007**, *129*, 15156–15163.
(57) Cairo, C. W.; Gestwicki, J. E.; Kanai, M.; Kiessling, L. L. *J. Am. Chem. Soc.* **2002**, *124*, 1615–1619.
(58) Ladmiral, V.; Mantovani, G.; Clarkson, G. J.; Cauet, S.; Irwin, J. L.; Haddleton, D. M. *J. Am. Chem. Soc.* **2006**, *128*, 4823–4830.
(59) Yang, Q.; Hu, M.-X.; Dai, Z.-W.; Tian, J.; Xu, Z.-K. *Langmuir* **2006**, *22*, 9345–9349.
(60) Bouckaert, J.; Berglund, J.; Schembri, M.; De Genst, E.; Cools, L.; Wuhrer, M.; Hung, C.-S.; Pinkner, J.; Slaettegard, R.; Zavialov, A.; Choudhury, D.; Langermann, S.; Hultgren, S. J.; Wyns, L.; Klemm, P.; Oscarson, S.; Knight, S. D.; De Greve, H. *Mol. Microbiol.* **2005**, *55*, 441–455.